NEW RESULTS IN MESON SPECTROSCOPY FROM THE CRYSTAL BARREL EXPERIMENT

Curtis A. Meyer
Carnegie Mellon University, Pittsburgh, PA 15213

The Crystal Barrel Collaboration

ABSTRACT

Recent observations by the Crystal Barrel experiment of two scalar resonances, $f_0(1365)$ and $a_0(1450)$ have allowed us to clarify the members of the scalar nonet. In addition, a third scalar, $f_0(1500)$, appears to be supernumerary, and is a candidate for the scalar glueball expected near 1500 MeV.

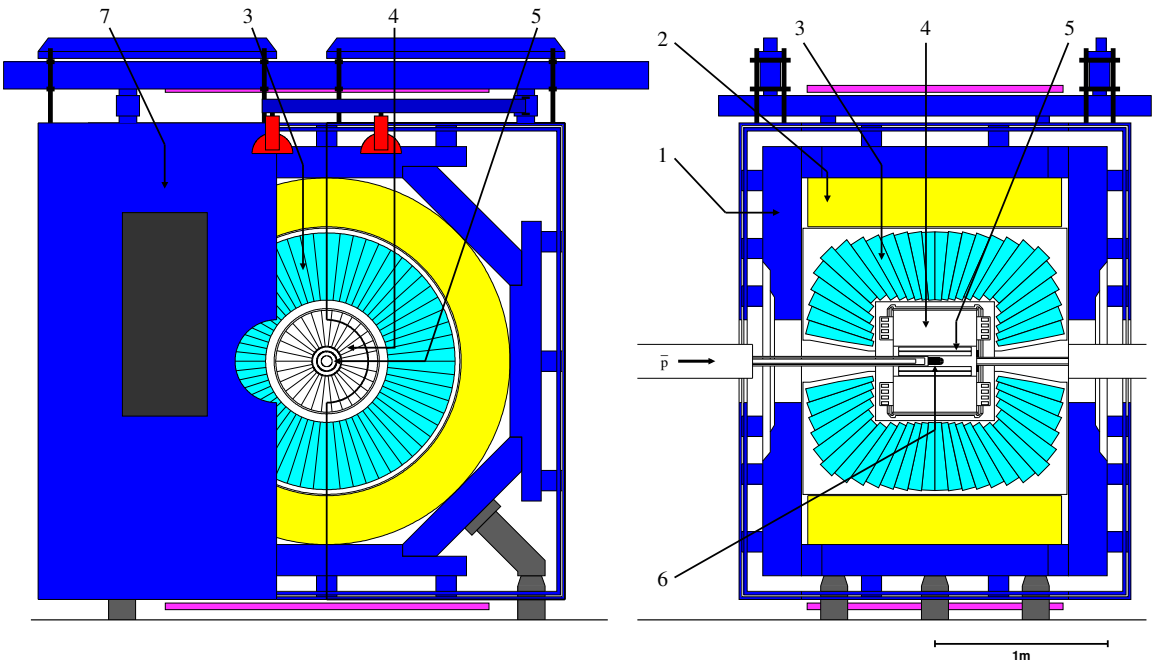

Figure 1: The Crystal Barrel detector. Magnet yoke (1), magnet coils (2), CsI–calorimeter (3), JDC (4), PWC (5), target (6), one half of the endplate (7).

1. The Crystal Barrel Detector

The Crystal Barrel detector at LEAR [1] is a nearly 4π apparatus for both charged particles and photons. The detector is used to study $\bar{p}p$ annihilation at rest and in flight, (up to 1.9GeV/c), and has been very productive in the field of meson spectroscopy. In particular, the scalar nonet, $J^{PC} = 0^{++}$ is now much better understood, and a good candidate for the scalar glueball now exists.

The detector is shown in Fig. 1. The antiprotons enter along the axis of the 1.5 T

solenoidal field, and stop in a liquid hydrogen target. They annihilate, and the resulting $\pi^{\pm}$, $K^{\pm}$ and γ's are tracked outward through the detector. Immediately outside the hydrogen target are two cylindrical multiwire proportional chambers used to either trigger on or veto events with charged particles. Next is a 23 layer cylindrical drift chamber, (JDC). The chamber is divided axially into 30 sectors, with an 8mm wire spacing between adjacent radial layers. The wires are read out at each end to provide a z–measurement through charge division. Outside the JDC is the CsI(Tl) barrel built with 1380 16 radiation length crystals. The crystals are arranged in a center–pointing geometry, and the calorimeter has achieved an energy resolution of 2.5% at 1GeV.

2. New Results

The data discussed in this paper come from two triggers; the all–neutral trigger, (no charged particles in the PWC), and the minimum–bias trigger, (a $\bar{p}$ entering the liquid hydrogen target). The 6γ final state is obtained from $16.8 \cdot 10^6$ all neutral annihilations at rest, while the $\pi^+\pi^-\pi^\circ\pi^\circ\pi^\circ$ data are from $3.8 \cdot 10^6$ minimum–bias events. In the 6γ final state, we reconstruct $\bar{p}p \to \pi^\circ\pi^\circ\pi^\circ$ (712k events), $\bar{p}p \to \pi^\circ\pi^\circ\eta$ (187k events), $\bar{p}p \to \pi^\circ\eta\eta$ (31k events), and $\bar{p}p \to \pi^\circ\eta\eta'$ (130 events), where π°, η and η' are all detected in their 2γ decay modes. These data have been analyzed using two different methods, the K–matrix formalism [2] and the N/D method [3]. Both methods use a coupled channel approach, allowing both $\pi\pi$ or $\eta\eta$ and an unseen $K\bar{K}$ decay.

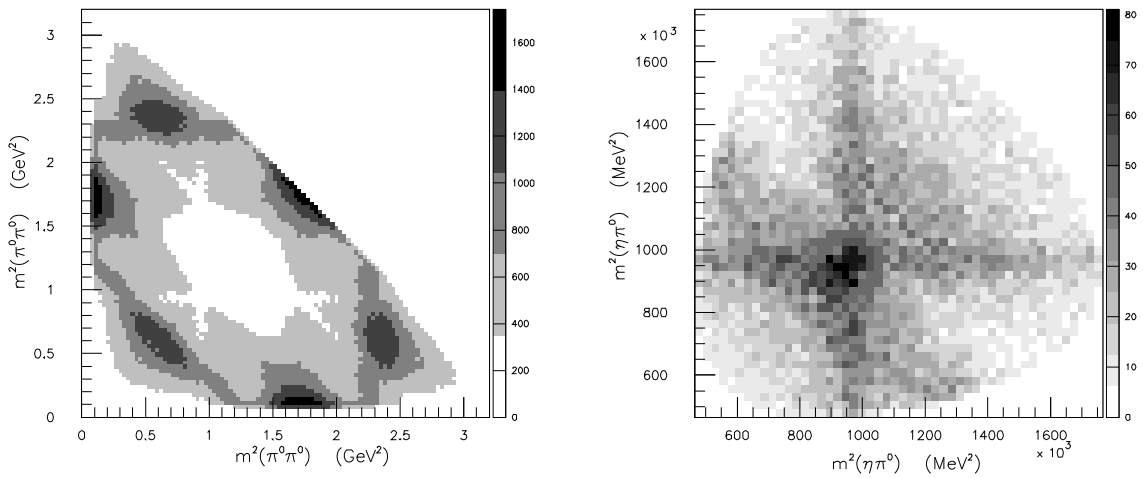

Figure 2: The Dalitz plots for $\bar{p}p \to \pi^\circ\pi^\circ\pi^\circ$ (left) and $\pi^\circ\eta\eta$ (right).

The $\bar{p}p \to \pi^\circ\pi^\circ\pi^\circ$ Dalitz plot (Fig. 2–left) has 3–fold symmetry, meaning that resonances are seen simultaneously as three bands, vertical, horizontal and diagonal. In the vertical, one sees a band near 0.9 GeV^2 corresponding to the $f_0(975)$. The two blobs at the upper and lower edge of the plot near 1.7 GeV^2 corresponds to the $f_2(1270)$, and the vertical band near 2.25 GeV^2 corresponds to a new scalar resonance, the $f_0(1500)$. The blob near 2.4 GeV^2 is caused by reflections from the low–mass $\pi\pi$ system, and a tensor state, ($J^{PC} = 2^{++}$) near 1550 MeV. In addition, the fit to this

Dalitz plot requires a broad, inelastic scalar state at a mass of 1365 MeV, which is probably the $f_0(1400)$.

The $\eta\eta\pi^\circ$ Dalitz plot has a 2–fold symmetry. Resonances in the $\eta\pi^\circ$ system are seen as horizontal and vertical bands, while resonances in the $\eta\eta$ system are seen as diagonal bands. The Dalitz plot , (Fig. 2–right) shows a clear signal for the $a_0(980) \to \eta\pi^\circ$ as the horizontal and vertical crossing bands near $950 \cdot 10^3$ MeV^2. In addition, there are two diagonal bands corresponding to the $f_0(1365) \to \eta\eta$ and the $f_0(1500) \to \eta\eta$. A simultaneous spin–parity analysis [4] of both $\pi^\circ\pi^\circ\pi^\circ$ and $\eta\eta\pi^\circ$ yields the following parameters for the two isoscalar scalar resonances. (Note: we indicate a mass of 1500 for the second f_0 because a second analysis leads to a mass between 1480 and 1520.)

$$f_0(1365) \quad m = 1365^{+20}_{-55} \quad \Gamma = 267 \pm 70$$
$$f_0(1500) \quad m = 1520 \pm 25 \quad \Gamma = 148^{+20}_{-25}$$

The Dalitz plot for $\bar{p}p \to \eta\pi^\circ\pi^\circ$ (Fig. 3–left), exibits a very complicated interference pattern which is evidence for dominance of a single initial state. This is confirmed by a spin–parity analysis [5] of these data coupled to $\pi^\circ\pi^\circ\pi^\circ$ and $\eta\eta\pi^\circ$. The $\eta\pi^\circ\pi^\circ$ final state arises almost entirely from the $^1S_0$ state of the $\bar{p}p$ atom. The analysis explains the data using the following amplitudes. [$\pi\pi$ S–wave] Including the AMP

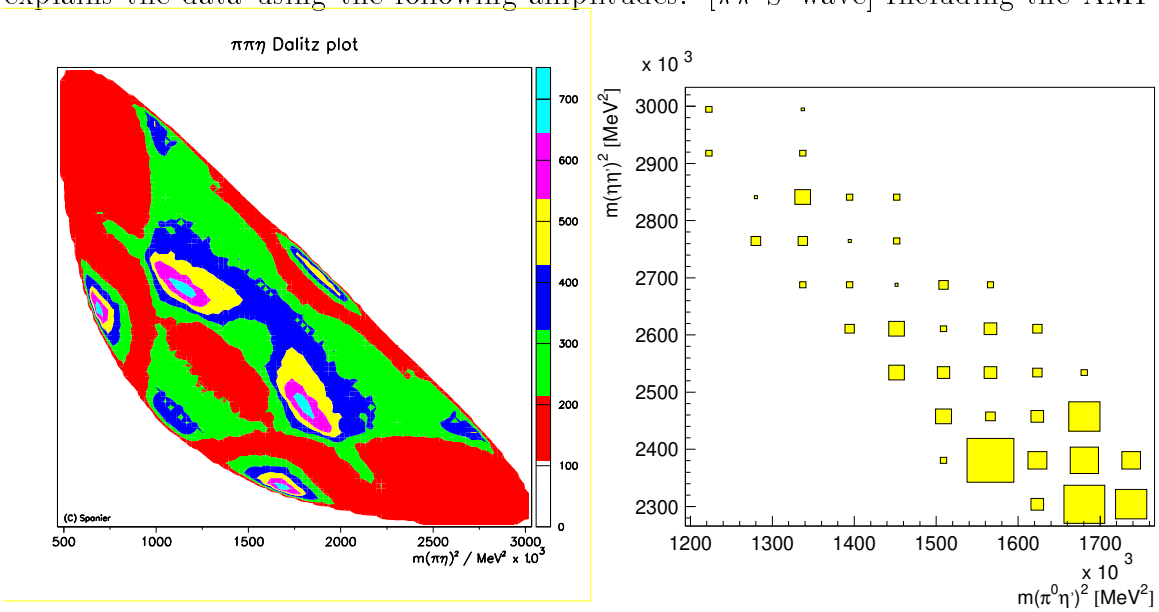

Figure 3: The Dalitz plots for $\bar{p}p \to \pi^\circ\pi^\circ\eta$ (left) and $\eta'\eta\pi^\circ$ (right).

parametrization [6], $f_0(975)$ and $f_0(1365)$ explain 50 to 55% of the data. [$\pi\eta$ S–wave] The $a_0(980)$ explains 13 to 15% of the data. In addition the data demand a second resonance, the $a_0(1450)$ which explains 5% of the data. Ignoring the second resonance causes the χ^2/N_{dof} to increase from 1.2 to 2.5. [$\pi\eta$ P–wave] A broad non–resonant background wave is needed to explain about 1.5 to 4.5% of the data. We exclude a resonance interpretation with the mass and width reported by GAMS for the $\hat{\rho}(1405)$ [7]. [$\eta\pi$ d–wave] The $a_2(1320)$ describes 18 to 28% of the data. In addition, a second a_2

is needed to account for about 2% of the data. However, its mass is at the edge of phase space, and we do not claim that this is a resonance.

The Dalitz plot for $\bar{p}p \to \eta'\eta\pi^\circ$ is shown in Fig. 3–right. Of the 158 events in this plot, 28 are estimated to be from background distributed uniformly over the plot. The enhancement in the lower right corner of the plot is most likely a structure in the $\eta'\eta$ system. A spin parity analysis is currently under way to determine if this is the $f_0(1500) \to \eta'\eta$.

The system $\bar{p}p \to \pi^+\pi^-\pi^\circ\pi^\circ\pi^\circ$ has been examined to search for resonances decaying into $\rho^+\rho^-$ [8]. The mass–mass plot, (Fig. 4–right) shows an enhancement in the $\rho^+\rho^-$ data over the background. The analysis of these data show the presence of a scalar resonance X decaying into $\rho\rho$ and $\sigma\sigma$, where σ is the $\pi\pi$ s–wave as given by the AMP parametrization [6]. We find $m_X = 1374 \pm 38$ MeV and $\Gamma_X = 375 \pm 61$ MeV. Under the assumption that this is isoscalar, it is probably the inelastic $f_0(1365)$ seen above, and we estimate that its 4π:2π decay ratio is approximately 5:1.

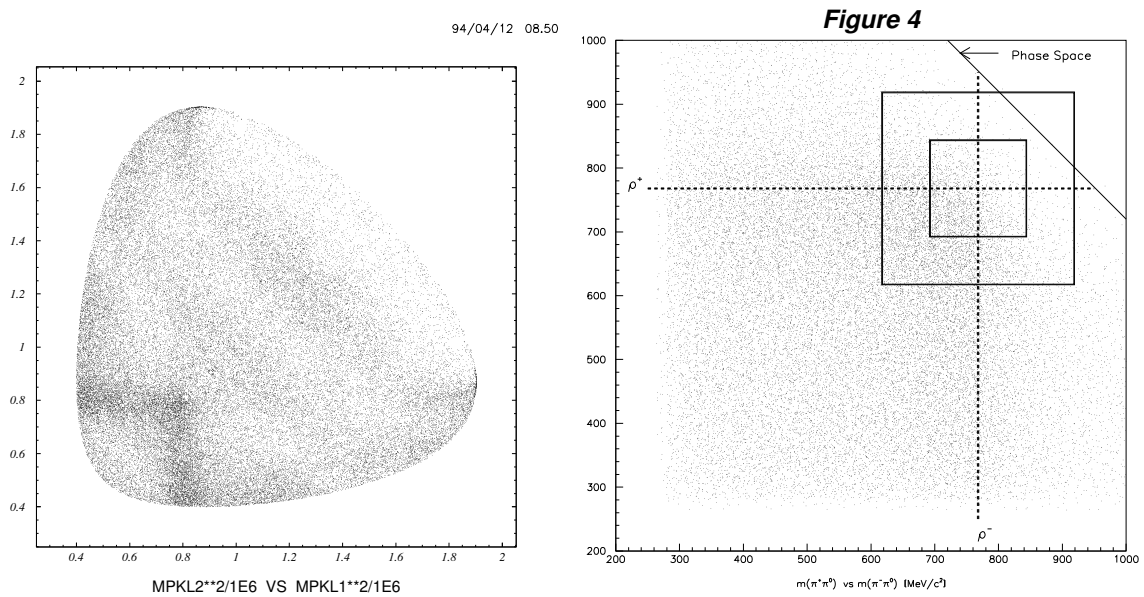

Figure 4: The Dalitz plots for $\bar{p}p \to \pi^\circ K_L K_L$ (left) and the mass–mass plot from $\pi^+\pi^-\pi^\circ\pi^\circ\pi^\circ$.

Finally, the $K\bar{K}\pi^\circ$ final state is very important in classifying mesons. In Fig. 4–left is shown a very preliminary Dalitz plot for the $K_L K_L \pi^\circ$ final state. The $K^*(890)$ can be seen as crossing horizontal and vertical bands near 0.8 GeV^2. In addition, there are hints of three diagonal bands ($K_L K_L$ resonances). A spin parity analysis to determine if any of these bands are 0^{++} is still underway. However, this analysis will be unable to distinguish between isospin 0 and 1.

3. The Scalar Nonet

In Table 1 are shown the ground state $L = 1$ nonets in the quark model as assigned by the Particle Data Group [9]. Normally, the octet and singlet $I = 0$ members of the nonets are mixed. The mixing angle can be computed from the Gell-mann Okubo formula, where Θ_q is from the quadratic formula, and Θ_l is from the linear formula. In the case of an ideally mixed nonet, (complete separation between the $u\bar{u} + d\bar{d}$ and the $s\bar{s}$ components), $\Theta = 35.3°$. In table 1 are given the two mixing angles for the PDG assignments for all except the scalars. Most of these are fairly close to ideally mixed.

$^{2S+1}L_J$ J^{PC}	$I = 1$ $u\bar{d}$, $u\bar{u}$, $d\bar{d}$	$I = 0$ $u\bar{u}$, $d\bar{d}$,		$I = 0$ $s\bar{s}$		$I = 1/2$ $\bar{s}u$, $\bar{s}d$	Θ_q (Θ_l)
$^1P_1$	$b_1(1235)$	$h_1(1170)$,		$h_1'(1380)$		$K_1(1270)$	41°
1^{+-}	$\Gamma = 155$	$\Gamma = 360$,		$\Gamma = 80$	$K\bar{K}^*$	$K_1(1400)$	(40°)
$^3P_0$	$a_0(980)$	$f_0(975)$,		$f_0(1400)$		$K_0^*(1430)$	
0^{++}	$\Gamma = 57$	$\Gamma = 47$,	20% $K\bar{K}$	$\Gamma = 400$	93% $\pi\pi$	$\Gamma = 287$	
$^3P_1$	$a_1(1260)$	$f_1(1285)$,		$f_1(1510)$		$K_1^*(1400)$	38°
1^{++}	$\Gamma = 400$	$\Gamma = 25$,	$K\bar{K}^*$	$\Gamma = 35$	10% $K\bar{K}$	$K_1(1270)$	(36°)
$^3P_2$	$a_2(1320)$	$f_2(1270)$,		$f_2'(1525)$		$K_2(1430)$	31°
2^{++}	$\Gamma = 110$	$\Gamma = 185$,	5% $K\bar{K}$	$\Gamma = 85$	71% $K\bar{K}$	$\Gamma = 105$	(29°)
New 0^{++} Assignment							
$^3P_0$	$a_0(1450)$	$f_0(1365)$,		$f_0(1520)$		$K_0^*(1430)$	49°
0^{++}	$\Gamma = 250$	$\Gamma = 267$,	$\approx$70% 4π	$\Gamma = 80$	$K\bar{K}$	$\Gamma = 287$	(48°)

Table 1: The $L = 1$ mesons shown with their widths and some decay fractions.

Looking at the 0^{++} assignment, it is fairly clear that the $a_0(980)$ and the $f_0(975)$ do not fit well into the nonet. Other evidence from both two–photon couplings and J/ψ decays indicate that these states are not simple $q\bar{q}$ systems. Given that these are not members of the scalar nonet, what are the members? The $f_0(1365)$, (probably the $f_0(1400)$), is a good candidate for the lightest $I = 0$ member. In addition the $a_0(1450)$ fits naturally in as the $I = 1$ member. There are now three possible candidates for the $I = 0$ mostly $s\bar{s}$ member. The Crystal Barrel $f_0(1500)$, the LASS $f_0(1520)$ [10] and the GAMS $f_0(1590)$ or G meson [11]. Given that that $f_0(1365)$ and $a_0(1450)$ are very similar in mass, we expect the last member to be mostly $s\bar{s}$, with strong couplings to $K\bar{K}$. The decays of the $f_2'(1525)$ can guide us: $K\bar{K}$ 71%, $\eta\eta$ 28% and $\pi\pi$ 1%. Crystal Barrel observes no strong $K\bar{K}$ signal for the $f_0(1500)$, which probably rules this state out. The LASS state is observed in $K\bar{K}$, while the GAMS state is seen to decay into $\eta'\eta$, $\eta\eta$ and $4\pi°$. If we assume that the LASS state is the missing member, then we will fill out the scalar nonet as in the last column of table 1.

This leaves the $f_0(1500)$ and $f_0(1590)$ as extra scalar states — what are they? Earlier analysis of the $\eta\eta\pi$ by Crystal Barrel found the $f_0(1500)$ at a mass of 1560 MeV [12]. Coupled channel analysis as well as better analysis procedure have shifted the mass down to the 1500 MeV value. While the GAMS state is seen to decay most strongly

to $\eta'\eta$, Crystal Barrel places an upper limit on $\eta\eta$:$\eta'\eta$ of 4:1. It seems unlikely that these are the same states.

Lattice calculations predict that the lowest mass scalar glueball should have a mass around 1500 MeV. In addition, the decay modes for a glueball are expected to be flavor blind. If we assume that the enhancement seen in the $\eta'\eta$ invariant mass is indeed the $f_0(1500)$, then from the Crystal Barrel data, one can extract the following production and decay ratios [13].

$$\begin{aligned} BR(\bar{p}p \to \pi^\circ f_0(1500), f_0(1500) \to \pi\pi) &= (38 \pm 10.0) \cdot 10^{-4} \\ BR(\bar{p}p \to \pi^\circ f_0(1500), f_0(1500) \to \eta\eta) &= (6.3 \pm 2.8) \cdot 10^{-4} \\ BR(\bar{p}p \to \pi^\circ f_0(1500), f_0(1500) \to \eta'\eta) &= (1.5 \pm 0.5) \cdot 10^{-4} \end{aligned}$$

These have been corrected for the 2γ decay modes, and the isospin of the π. In order to identify the $f_0(1500)$ as a scalar glueball, it will be necessary to see its $K\bar{K}$ decay. This is currently under investigation, as evidenced by the K_LK_L data above. In addition, a specials K_SK_S trigger will be brought online at the end of '94. From bubble chamber results for $\bar{p}p \to \pi^\circ K\bar{K}$ [14], one can obtain an upper limit for $f_0(1500) \to K\bar{K}$. This then leads to the following decay pattern:

$$f_0(1500) \to \pi\pi : \eta\eta : \eta'\eta : K\bar{K} = 3 : (0.72 \pm 0.37) : (1.05 \pm 0.44) :< 0.40$$

which is very suggestive of the flavor blind decay of a glueball, but without information of the $K\bar{K}$ decay mode it is very difficult to confirm this. In addition, the preliminary results still await the completion of the ongoing spin–partity analysis, and the planned collection of $K\bar{K}\pi$ data at the end of '94.

4. References

1. E. Aker *et al.*, **Nucl. Instrum. Methods A321**, 69, (1992).
2. S. U. Chung, *et al.*, submitted to **Z. Phys. C**, (1994).
3. D. V. Bugg, *et al.*, submitted to **Phys. Rev. D.**, (1994).
4. V. V. Anisovich, *et al.*, **Phys. Lett. B323**, 233, (1994).
5. C. Amsler, *et al.*, Submitted to **Phys. Lett. B**, (1994).
6. K. L. Au, D. Morgan and M. R. Pennington, **Phys. Rev. D35**, 1633, (1987).
7. M. Boutemeur and M. Poulet, Hadron 89, ed. F. Binon, J. M. Frère, J. P. Peigneux – (Ed. Frontiérs 1989), p.119.
8. C. Amsler, *et al.*, **Phys. Lett. B322**, 431, (1994).
9. K. Hikasa, *et al.*, **Phys. Rev. D45 II**, (1992).
10. D. Aston *et al.*, **Nucl. Phys. B301**, 525, (1988).
11. F. Binon *et al.*, **Nuovo Cimento 78A**, 313, (1983), and **80A**, 303, (1984).
12. C. Amsler *et al.*, **Phys. Lett. B291**, 347, (1992).
13. R. Hackmann, Proceedings of the Recontre de Moriond, (1994).
14. L. Gray *et al.*, **Phys. Rev. D27**, 307, (1983).